DESIGN, SYNTHESIS AND CHARACTERIZATION OF PEPTIDE-GUIDED NANOMATERIAL FOR CANCER TARGETING

An Undergraduate Research Scholars Thesis

by

MEGAN METCALF

Submitted to the Undergraduate Research Scholars program at
Texas A&M University
in partial fulfillment of the requirements for the designation as an

UNDERGRADUATE RESEARCH SCHOLAR

Approved by Research Advisors: Dr. Hong-Cai Zhou

May 2018

Major: Chemistry

TABLE OF CONTENTS

ABSTRACT

Design, Synthesis and Characterization of Peptide-Guided Nanomaterial for Cancer Targeting

Megan Metcalf
Department of Chemistry
Texas A&M University

Research Advisor: Dr. Hong-Cai Zhou
Department of Chemistry
Texas A&M University

Specifically targeting cancer cells is much more efficient than non-targeted treatment because it decreases side effects and permits stronger treatment without as a risk of harming normal cells. Smart molecular probes and materials capable of passively or actively targeting cancerous cells show potential in cancer treatment for this reason. The combination of Metal-Organic Frameworks (MOFs) with actively targeting molecules provides an attractive way for targeted cancer theranostic methods. In this work, peptide sequences were synthesized that have high affinity and specificity towards proteins expressed on the surface of cancer cells. To introduce enough flexibility for targeted binding and provide extra functionality, the targeting peptide AP2H was further modified with polyethylene glycol (PEG) as a spacer molecule, and the peptide RGDG was used in place of RGD in order to use the additional glycine residue as a spacer molecule. After solid phase synthesis and cleavage, the resultant peptides were characterized with high-performance liquid chromatography (HPLC) and mass spectrometry (MS). Biocompatible metal-organic frameworks ZIF-8, UiO-66, and UiO-66-NH_2 were synthesized. UiO-66-NH_2 was functionalized with the peptide sequences to build a targetable

delivery system using the MOF to carry molecules, such as fluorescent probes or anticancer drugs, directly to tumor cells by using the targeting peptides RGD and AP2H.

Doxorubicin (DOX), a typical anticancer drug, was used as a model to determine whether the peptide-guided delivery system has the potential for carrying molecular cargos. UV-Vis spectrophotometry was used to quantitatively measure the uptake and subsequent release of DOX. The DOX-encapsulated MOF paired with a targeting peptide can be promising as a targetable delivery system for cancer treatment.

ACKNOWLEDGEMENTS

I would like to thank my research advisor, Dr. Hong-Cai Zhou for the opportunity to work with the Zhou research group for the last two years. It has been a great experience.

Thanks to Dr. Yanyan Huang for her guidance and patience throughout the research. Dr. Huang's help has been essential to the completion of the project.

Thanks go to the entire Zhou research group for always being ready to answer questions when they arise.

This work was supported by the Welch Foundation through a Robert A. Welch Endowed Chair in Chemistry to H.J.Z. (A-0030).

ABBREVIATIONS

MOF	Metal-Organic Framework
RGDG	RGDG amino acid sequence
AP2H	IHGHHIISVG amino acid sequence
PEG	polyethylene glycol
LAPTM4B	lysosomal protein transmembrane 4 beta
DOX	doxorubicin
HPLC	High Performance Liquid Chromatography
SEM	Scanning Electron Microscopy
MS	Mass Spectrometry
TFA	trifluoroacetic acid
TIS	triisopropylsilane
SA	succinate anhydride
PBS	phosphate buffered saline
CDI	1,1'- carbonyldiimidazole
HBTU	(2-(1*H*-benzotriazol-1-yl)-1,1,3,3-tetramethyluronium hexafluorophosphate

CHAPTER I

INTRODUCTION

Cancer, as a global threat to public health, has warranted extensive attention from researchers in a variety of fields. Chemotherapy is one of the most important treatments for cancer but is still challenged by its severe side effects to healthy cells due to the lack of selectivity. To address this, targetable chemical probes and materials for precise cancer diagnosis and treatment are critically needed.

Proteins specifically overexpressed on cancer cells are excellent targets for cancer treatment and have been explored as targets for the development of cancer-detecting bioprobes. These probes are required to exhibit high affinity, selectivity, and sensitivity for their target proteins.[1] Nowadays, increasingly more peptides are discovered that recognize cancer-related molecular events. For example, RGD is a well-known tripeptide sequence which can specifically bind integrin $\alpha_v\beta_3$, a transmembrane protein commonly overexpressed in cancer cells. Due to the critical role of integrin $\alpha_v\beta_3$ in regulating tumor growth and metastasis, various RGD-based probes have been developed for cancer analysis.[2,3] Recently, the decapeptide AP2H has been reported to recognize a tumor-related protein, lysosomal protein transmembrane 4 beta (LAPTM4B), and has increased affinity for LAPTM4B in the characteristic low-pH environment of tumor cells.[1,4]

Metal-Organic Frameworks (MOFs) are a class of porous coordination polymers composed of inorganic building blocks with organic linkers. The tunability of MOFs in morphology, size, and porosity allows flexibility in synthesizing nanomaterials with a desired function. The highly porous structure of MOFs makes them attractive carriers for different

molecules, such as imaging agents and chemotherapeutics.[5-8] For biomedical and analytical applications of MOFs, there are challenges including controlling size in nanoscale, biocompatibility, and stability in an aqueous environment. In addition, cell penetrability and non-specificity are also major concerns.

Herein, aimed at developing a targeted delivery nano-system for cancer treatment, cancer cell-targeting peptides were synthesized for the functionalization of MOFs. Two peptide sequences, RGD and AP2H, were chosen as the targeting vehicles. To introduce enough flexibility for cell binding and extra functionality, the AP2H peptide was further modified with a spacer, and the RGD peptide was lengthened to RGDG. The peptides were characterized via HPLC and MS. As the transporters, MOFs built from different metal ions and ligands were prepared. MOFs like ZIF-8 and UiO-66, which contain metal ions Zn(II) and Zr(IV) respectively, were chosen due to stability in water and safety of their metal ions in biological systems.[6-8] The size and morphology of the MOFs were observed with scanning electronic microscopy (SEM). The MOF UiO-66-NH_2 was synthesized for functionalization of the MOF with a targeting peptide sequence by making use of NH_2 groups on the ligands of the MOF. The coupled MOF and targeting peptide are designed to function as the aforementioned nanoscale delivery system, with the targeting peptide guiding the MOF and its cargo directly to tumor cells.

Doxorubicin is an anticancer drug on the World Health Organization's list of essential medicines.[9] A potential cargo for the delivery system, doxorubicin (DOX), was chosen to test the system due to its fluorescent properties and well-known systemic toxicity. UV-Vis spectrophotometry was used to quantitatively determine the uptake and subsequent release of DOX from UiO-66 and UiO-66-NH_2.

CHAPTER II

METHODS

Synthesis.

Peptide synthesis.

Peptides were synthesized manually by the solid-phase FMOC synthesis approach, as shown in Scheme 1. An FMOC-Gly-Wang resin was used as the starting material in both peptides. The spacer molecule with AP2H, PEG, was also coupled while the peptide sequence remained on the resin. After cleavage, the products were obtained as solid powders.

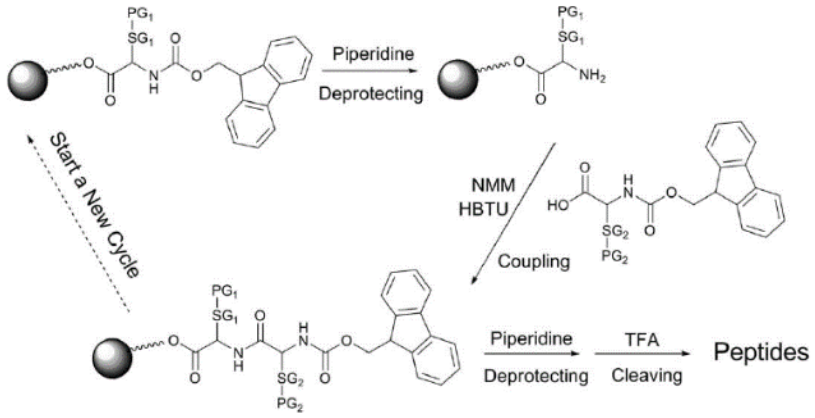

Scheme 1. FMOC solid phase synthesis procedure.

HBTU was used as the activating reagent. A 20% piperidine in DMF solution was used for removal of the FMOC temporary protecting groups. After the peptide sequence was assembled, cleavage of peptides from the resin and global side-chain deprotection were carried out with a freshly prepared TFA cocktail (95% TFA, 2.5% H_2O, and 2.5% TIS). The product was analyzed on a SHIMADZU HPLC system (Kyoto, Japan).

Modification of peptide AP2H.

The modification of the peptide sequence was carried out via on-resin synthesis. After the amino acids of AP2H were assembled, the FMOC group was removed and a 2-fold excess of PEG5 was added. After coupling and washing, a 3-fold excess of succinate anhydride (SA) was introduced. The resultant product was then cleaved from the resin with a freshly prepared TFA cocktail (95% TFA, 2.5% H_2O and 2.5% TIS).

Synthesis of ZIF-8.

ZIF-8 was synthesized according to reported procedures.[10] Briefly, methanolic stock solutions of $Zn(NO_3)_2$•$6H_2O$ (25 mM) and of 2-methylimidazole (mIm) (50 mM) were prepared. ZIF-8 was obtained by mixing 10 ml $Zn(NO_3)_2$ stock solution and 10 ml mIm stock solution for 30 minutes at room temperature.

Synthesis of UiO-66.

UiO-66 was synthesized using two different methods, according to reported procedures.[11] In the first method, zirconyl chloride octahydrate was used. Terephthalic acid (50 mg, 0.24 mmol) was dissolved in 1 ml of DMF. In a separate vial, zirconyl chloride octahydrate (21 mg, 0.066 mmol) was dissolved in 3 ml of DMF. The two solutions were mixed together in a scintillation vial, and acetic acid (300 µl) was added to the reaction mixture. The solution was heated at 85˚C for 18 h. This MOF was used for SEM.

In the second method, zirconium(IV) chloride was used. In a vial, 77 mg of $ZrCl_4$, 52 mg of terephthalic acid, 620 mg of benzoic acid, 6 mL of DMF, and 75 µL of concentrated HCl were combined. The solution was heated at 120˚C for 48 h.

Synthesis of UiO-66-NH_2.

UiO-66-NH_2 was synthesized by the same procedure as the second synthesis method for UiO-66 but using 2-aminoterephthalic acid in place of terephthalic acid.[11]

Coupling.

Coupling of UiO-66-NH_2 to RGDG.

The coupling of RGDG to the MOF was done by a three-step approach, outlined in Scheme 2. This approach attaches a carboxylic acid to the amine groups of the MOF, then attaches the N-terminal of the peptide to the carboxylic acid on the MOF in order to avoid possible side reactions involving the carboxylic acid group in the aspartic acid side chain of RGDG. First, 2.9 mg of SA, 5 µL of DIEA, and 0.1 mL of DMF were combined, then 5 mg of UiO-66-NH_2 and 0.4 mL of DMF was added and the solution was stirred overnight. In the second step, 1.2 mg of CDI and 3 µL of DIEA were added to the solution, which was then stirred 2 h. In the third step, 5 mg HBTU, 3 µL of DIEA, and 0.6 mL of a solution of RGDG in methanol were added along with 0.3 mL of DMF and the solution was stirred overnight. HPLC was used to compare relative concentrations of RGDG in the reaction solution before and after the coupling reaction.

Coupling of UiO-66-NH_2 to AP2H.

The coupling of AP2H to the MOF was done by a single step reaction, outlined in Scheme 2, which links the C-terminal of the amino acid chain to the amine groups on the MOF. To a vial, 9.8 mg of HBTU, 0.5 mL of AP2H in H_2O, and 0.4 mL of DMF were added, then 80 µL and 8 mg of UiO-66-NH_2 were added and the solution was stirred overnight. HPLC was used to compare relative concentrations of AP2H in the reaction solution before and after the coupling reaction.

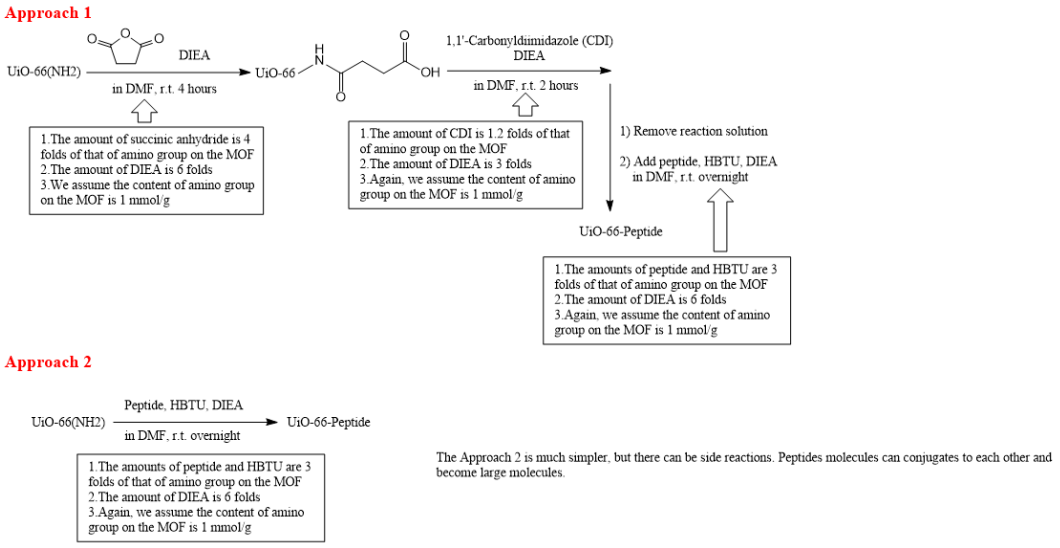

Scheme 2. Two approaches to coupling peptide to UiO-66-NH_2.

Doxorubicin Uptake.

A solution was prepared of 0.5 mg/mL of DOX in 10% DMF in PBS. In a vial, 1.5 mL of the DOX solution was added to 4.4 mg of UiO-66-NH_2. The solution was stirred for 2-3 days. The solution was then centrifuged, and supernatant removed to compare to the initial DOX solution. The MOF was washed with a 10% DMF in PBS solution for comparison with the initial DOX solution to determine DOX release from the MOF. The MOF was also washed with DMF after the PBS washes. The DOX uptake procedure and washes were repeated with UiO-66 instead of UiO-66-NH_2.

CHAPTER III

RESULTS

Synthesis.

Two peptides, RGD and AP2H with high affinity binding to cancer-related proteins were chosen as the targeting sequences. Their targets, integrin $\alpha_v\beta_3$ and LAPTM4B, are membrane anchored proteins, which are feasible targets for the recognition of cancer cells.[3,4] To avoid possible steric hindrance during the binding of peptides towards proteins, spacers were introduced to both peptide sequences. For RGD, an additional glycine was added in the carboxylic terminal to make RGDG. For AP2H, polyethylene glycol (PEG5) was incorporated.

The synthesized peptides RGDG, and AP2H-PEG5 were analyzed with HPLC and mass spectrometry. Given that AP2H has a longer sequence, it was also cleaved and characterized before the conjugation of PEG5 to ensure correct synthesis. The HPLC chromatograms and MS spectra are shown in Figure 1. By integrating the peak areas in the chromatograms, the purities of the peptides were calculated. The purity for RGDG is above 90%. AP2H and AP2H-PEG5 were both obtained with purities of around 80%. The appearance of m/z signals corresponding to the peptides in MS spectra demonstrates the success of the syntheses.

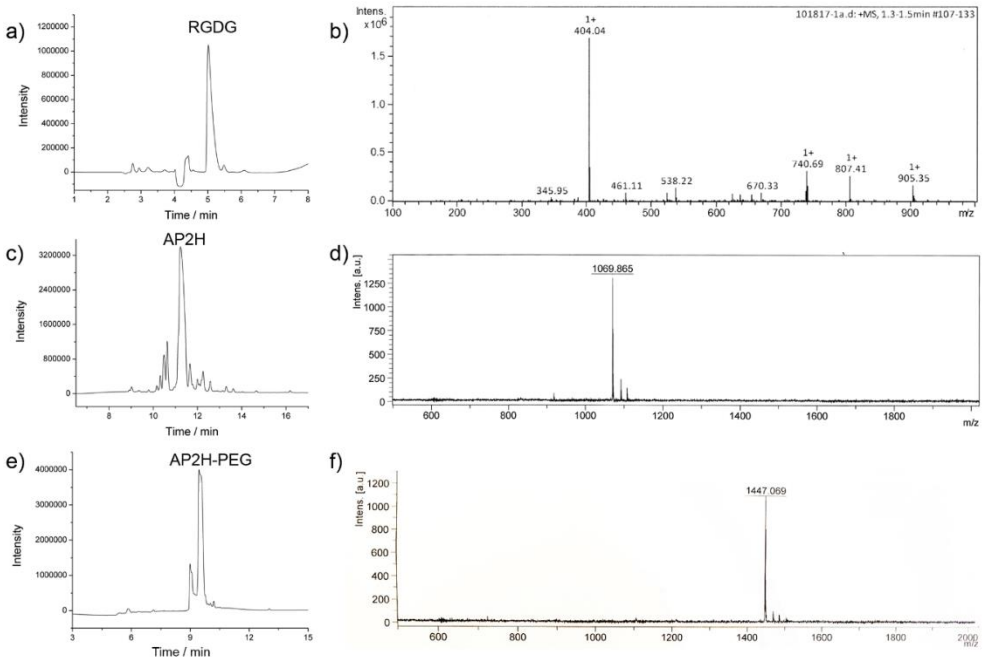

Figure 1. HPLC and MS analyses of peptides. (**a, c, e**) HPLC chromatograms of RGDG, AP2H and AP2H-PEG. (**b, d, f**) MS spectra of RGDG, AP2H and AP2H-PEG.

As the carrier of cargos into cancer cells, the MOFs should be stable and nontoxic in a physiological environment. Metal ions such as Zn(II) and Zr(IV) with high biocompatibility were chosen for the synthesis of ZIF-8 and UiO-66. As characterized with scanning electronic microscopy (SEM), the sizes of the MOFs are around 100 nm (Figure 2). The structure of UiO-66 is shown in Figure 3.

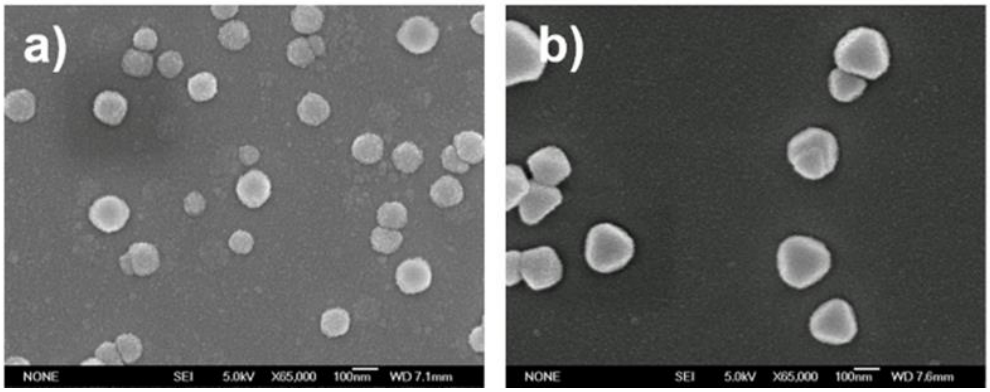

Figure 2. SEM images of ZIF-8 (a) and UiO-66 (b).

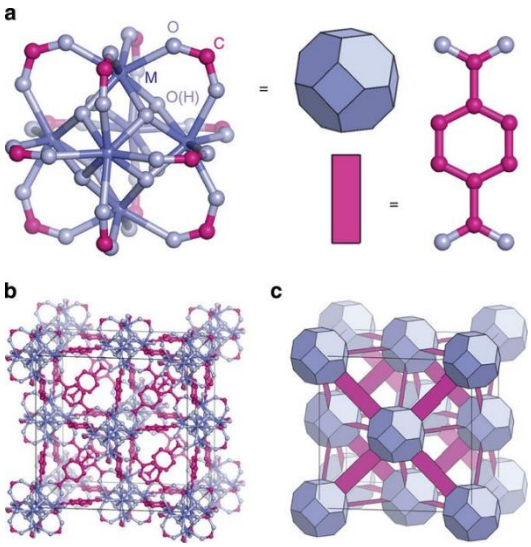

Figure 3. Shown in **a** is a fundamental building unit of UiO-66, a 6-center metal cluster with metal atoms in dark blue, oxygen in light blue, and carbon atoms in magenta. These clusters are connected by terephthalate linkers, shown on the right side of **a**. Demonstrated by **b**, UiO-66 takes on a face-centered cubic arrangement. A simplified version of the UiO-66 structure is shown in **c**.[12]

Coupling.

The nanoscale size of the MOFs can take advantage of the enhanced permeability and retention (EPR) effect in tumor vasculature, causing the MOF and its cargo to accumulate within tumor cells, which is appealing for passive targeting.[13] In preparation for functionalization with peptides, UiO-66-NH_2 was prepared with the same procedure as that of UiO-66, except 2-aminoterephthalic acid was used in place of terephthalic acid. The free amino groups on UiO-66-NH_2, from 2-aminoterephthalic acid molecules, can be accessed for modification with peptides.

The targeting peptide AP2H was combined with UiO-66-NH_2 in a single-step procedure. As shown in Figures 1 and 4, the peak representing AP2H in the HPLC chromatogram occurs at 12.5 minutes. This peak on the chromatogram of the solution obtained before coupling is smaller than that of the solution obtained after coupling with the MOF. The change in concentration of AP2H before and after the reaction could not be determined.

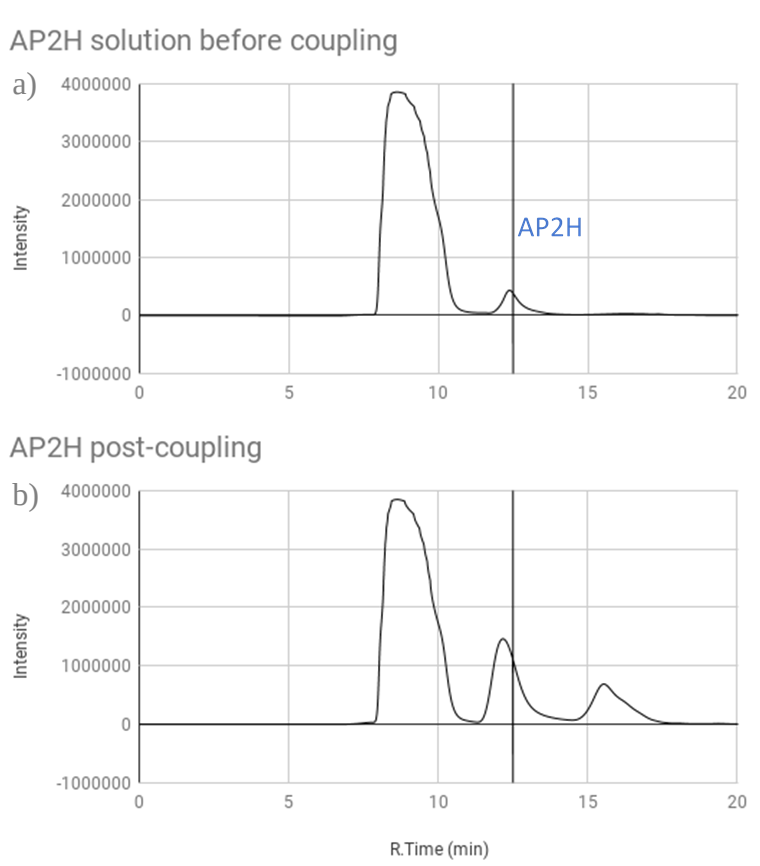

Figure 4. HPLC chromatograms of AP2H (**a**) before and (**b**) after the coupling reaction with reference lines at 12.5 minutes.

The targeting peptide RGDG was conjugated with UiO-66-NH_2 in a 3-step reaction. Firstly, UiO-66-NH_2 was modified with succinic anhydride to introduce carboxylic acid to the surface of the MOF, and then the N-terminal of the peptide was attached via peptide bond. RGDG was attached to the MOF via the amino group of arginine residue rather than the terminal glycine. This method can prevent the MOF from attaching to the carboxylic acid on the aspartic acid side chain and is controllable.

HPLC chromatograms of the RGDG solutions before and after the reaction were compared to determine the amount of RGDG that coupled to the MOF. The solutions collected

after washing the MOF were also analyzed with HPLC. The retention time of RGDG peptide in the HPLC chromatograms is 5 minutes, as shown in Figure 1. However, shown in Figure 5, there is no clear peak at 5 minutes for RGDG. Due to the presence of another component of the solution, it could not be determined whether there was a change in concentration of RGDG in solution.

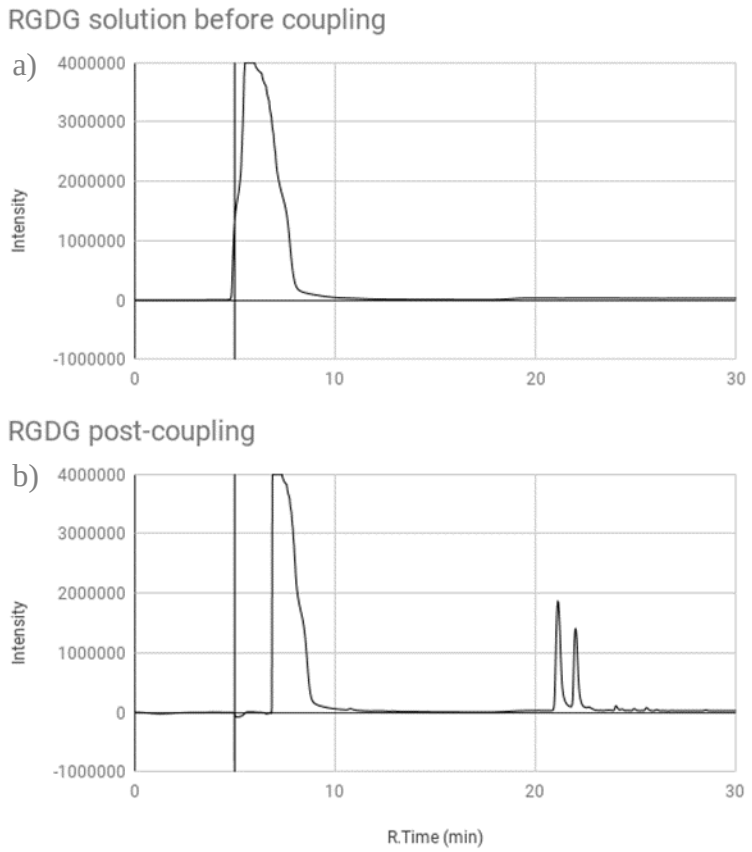

Figure 5. The HPLC chromatograms of RGDG (**a**) before and (**b**) after the coupling reaction with reference lines at 5 minutes.

Both the RGDG and AP2H coupling reactions had inconclusive results based on the HPLC chromatograms. This phenomenon may be due to some ligands or leftover reactants from

the MOF that washed out in the solution and overlapped with the peptide peaks in the chromatograms.

Doxorubicin Uptake.

The ability of UiO-66 and UiO-66-NH_2 to encapsulate and transport the anticancer drug DOX (Figure 6) was tested. DOX was chosen for its absorbance and fluorescent properties. And UV-Vis spectrophotometry was used to quantitatively determine doxorubicin uptake by the MOFs.

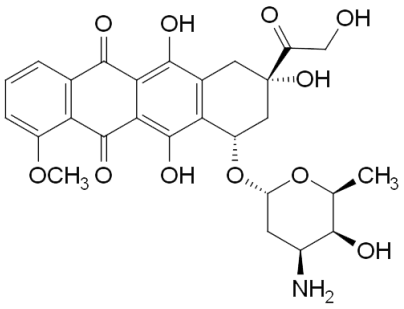

Figure 6. Doxorubicin (DOX) structure.

Stock solutions of varying concentrations of DOX (10% DMF in PBS) were prepared. UV-Vis spectra were obtained for each at 496 nm, which is the peak absorbance for DOX. As shown in Figure 7, the calibration curve has a trendline with the following equation, where A represents absorbance and c represents concentration:

$$A = 2.29 * c - 0.0138 \quad \text{(Eq. 1)}$$

The calibration curve is linear and consistent with Beer's law, as shown below, where L is path length and ε is the molar absorptivity constant.

$$A = \varepsilon * L * c \qquad \text{(Eq. 2)}$$

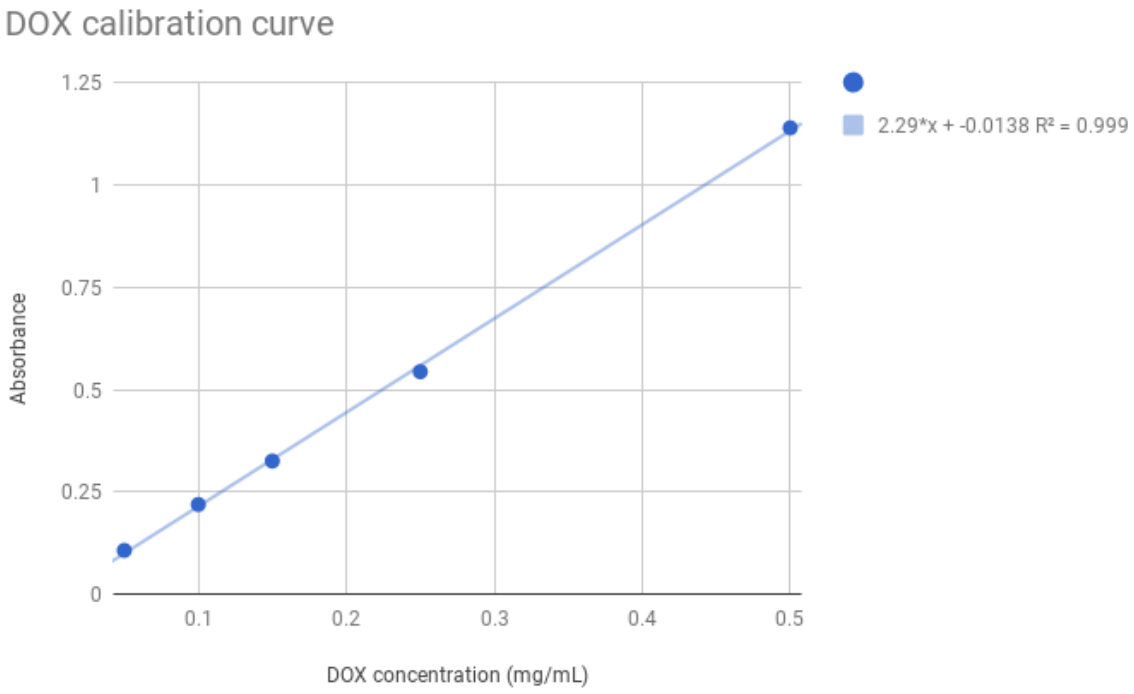

Figure 7. Calibration curve for DOX in PBS added with 10% DMF.

After mixing UiO-66 and UiO-66-NH_2 in 5 mg/mL DOX stock solution for varied periods (1.5 hours, 2 days and 3 days), the concentration of DOX remaining in each solution was measured and compared with the stock solution in order to determine encapsulation efficiency of each MOF, as shown in Table 1.

Table 1. DOX uptake by UiO-66-NH_2 and UiO-66.

MOF	**Mixing time**	**Absorbance at 496 nm**	**Concentration (mg/mL)**	**Mass remaining (mg)**	**Encapsulation efficiency**

UiO-66	2 days	0.503	0.23	0.34	95.5%
UiO-66-NH_2	2 days	0.432	0.19	0.29	96.1%
UiO-66-NH_2	3 days	0.121	0.06	0.09	98.8%
UiO-66-NH_2	1.5 hours	0.465	0.21	0.31	95.8%

Based on the encapsulation efficiencies of UiO-66-NH_2 after varying encapsulation times, shown in Table 1, it appears most of the DOX was encapsulated within the first hour and a half, while increasing encapsulation times increase encapsulation efficiency by only a small amount. This indicates that, despite the relatively large size of the DOX molecule compared to the ligand used to form the MOF, 2-aminoterephthalic acid, the uptake is very favorable and rapid.

Multiple washes were performed to examine the retention strength of the MOFs towards DOX. Eluted and released DOX from 6 successive washes with PBS (10% DMF), followed by 3 washes with DMF was determined with UV-Vis spectroscopy. The mass of DOX removed from the MOFs with each wash is listed in Figure 8.

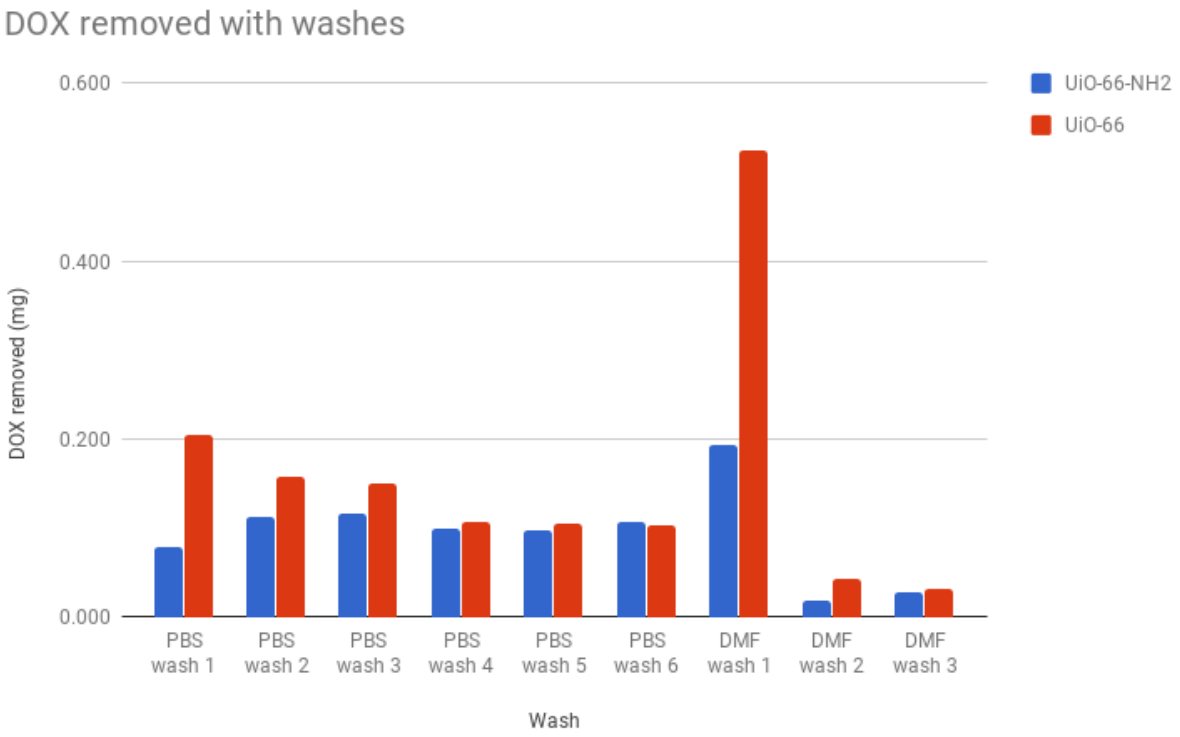

Figure 8. DOX removed from MOFs with PBS and DMF washes.

During the PBS washes, continuous release of DOX was detected, suggesting the weak adsorption of these DOX molecules on the MOFs. When the solvent was changed to DMF, a significant increase in DOX release was detected, especially for UiO-66. After the first DMF wash, almost none of the DOX was removed with subsequent washes. Most of the DOX that would come off with washes came off with the first DMF wash. As shown in Table 2, the washes removed only 12.8% of the DOX in UiO-66-NH_2, and 23.5% of the DOX in UiO-66. The total released amount of DOX is higher from UiO-66 than that from UiO-66-NH_2. This may be attributed to non-covalent interaction between DOX and amino groups on UiO-66-NH_2.

Table 2. DOX removal from MOFs after PBS and DMF washes.

MOF	DOX encapsulated (mg)	DOX removed (mg)	Percent removed	DOX removed with PBS washes (mg)	DOX removed with DMF washes (mg)	DOX remaining (mg)
UiO-66	6.992	1.427	23.5%	0.827	0.600	6.073
UiO-66-NH_2	7.368	0.848	12.8%	0.609	0.239	6.652

After DOX uptake by the MOFs, both UiO-66 and UiO-66-NH_2 changed color from white and pale yellow, respectively, to red as shown in Figure 9. DOX is a slightly darker color of red compared to the color of the MOF with DOX. After the washes, both MOFs retained the red color, as well as most of the DOX that had been encapsulated.

The MOFs retain much of the DOX encapsulated and encapsulate the DOX relatively quickly despite the size of the molecules. It is likely that the DOX interacted with UiO-66 and UiO-66-NH_2 quite strongly to form a different product. The UiO-66 and UiO-66-NH_2 both encapsulate DOX to a similar degree, indicating that the results are not exclusively due to the amino groups on UiO-66-NH_2. Instead, the DOX either reacted with a component of the MOFs unrelated to the ligand, or it was successfully taken into the pores of the MOF but could not easily be removed once there.

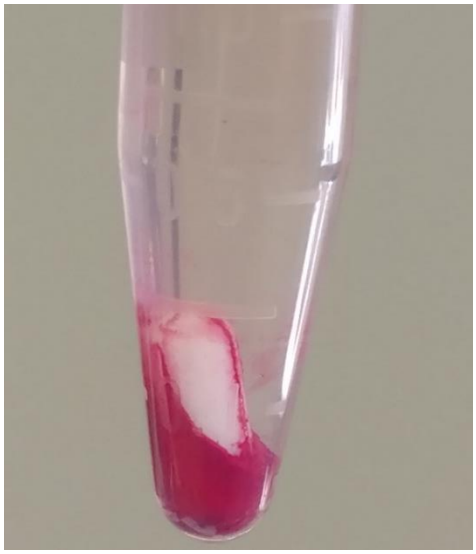

Figure 9. UiO-66-NH_2 after DOX uptake.

CHAPTER IV

CONCLUSION

Cancer cell-targeting peptides RGDG and AP2H were successfully synthesized and characterized. Biocompatible MOFs ZIF-8 and UiO-66 were also prepared with a size of around 100 nm, which is appealing for biomedical applications.

UiO-66-NH_2 with free amino groups was prepared for coupling to targeting peptide sequences. The NH_2 groups on the MOF are available for covalent functionalization with targeting peptides. HPLC chromatograms obtained of the reaction solution before and after peptide coupling were inconclusive due to compounds in solution overlapping with the peptide peak. Doxorubicin, a fluorescent anticancer drug, was used to test the uptake of UiO-66-NH_2, and therefore test a potential cargo for the peptide-guided delivery system. DOX was successfully absorbed by the porous MOFs with an encapsulation efficiency of 96.1%. The DOX was removed by washing the MOF, but only 12.8% of the DOX taken up by UiO-66-NH_2 could be removed.

With the guidance of cancer-cell targeting peptides, cargos encapsulated in MOFs can be delivered specifically to cancer cells. The selective targeting of cancer cells is beneficial to sensitive detection or specific ablation of cancer, while circumventing serious side effects to normal cells.

Future directions may include investigation of the concept with a variety of other cancer-targeting peptides and other bio-compatible MOFs. In addition, using cancer-targeting peptides may open up other options for cancer probes or anticancer drugs that would not be viable for less precise delivery methods.

REFERENCES

(1) Hu, F.; Huang, Y.; Zhang, G.; Zhao, R.; Yang, H.; Zhang, D. Targeted Bioimaging and Photodynamic Therapy of Cancer Cells with an Activatable Red Fluorescent Bioprobe. *Anal. Chem.* **2014**, *86*, 7987-7995.

(2) Dijkgraaf, I.; Kruijtzer, J. A. W.; Frielink, C.; Corstens, F. H. M.; Oyen, W. J. G.; Liskamp, R. M. J.; Boerman, O. C. αvβ3 Integrin-targeting of intraperitoneally growing tumors with a radiolabeled RGD peptide. *International Journal of Cancer* **2007**, *120*, 605-610.

(3) Shi, H.; Liu, J.; Geng, J.; Tang, B. Z.; Liu, B. Specific Detection of Integrin alpha(v)beta(3) by Light-Up Bioprobe with Aggregation-Induced Emission Characteristics. *J. Am. Chem. Soc.* **2012**, *134*, 9569-9572.

(4) Huang, Y. Y.; Zhao, R.; Fu, Y. B.; Zhang, Q. D.; Xiong, S. X.; Li, L.; Zhou, R. L.; Liu, G. Q.; Chen, Y. Highly Specific Targeting and Imaging of Live Cancer Cells by Using a Peptide Probe Developed from Rationally Designed Peptides. *ChemBioChem* **2011**, *12*, 1209-1215.

(5) Park, J.; Jiang, Q.; Feng, D.; Mao, L.; Zhou, H.-C. Size-Controlled Synthesis of Porphyrinic Metal-Organic Framework and Functionalization for Targeted Photodynamic Therapy. *J. Am. Chem. Soc.* **2016**, *138*, 3518-3525.

(6) Park, J.; Jiang, Q.; Feng, D. W.; Zhou, H. C. Controlled Generation of Singlet Oxygen in Living Cells with Tunable Ratios of the Photochromic Switch in Metal-Organic Frameworks. *Angew. Chem.-Int. Edit.* **2016**, *55*, 7188-7193.

(7) He, C. B.; Lu, K. D.; Liu, D. M.; Lin, W. B. Nanoscale Metal-Organic Frameworks for the Co-Delivery of Cisplatin and Pooled siRNAs to Enhance Therapeutic Efficacy in Drug-Resistant Ovarian Cancer Cells. *J. Am. Chem. Soc.* **2014**, *136*, 5181-5184.

(8) Alsaiari, S. K.; Patil, S.; Alyami, M.; Alamoudi, K. O.; Aleisa, F. A.; Merzaban, J. S.; Li, M.; Khashab, N. M. Endosomal Escape and Delivery of CRISPR/Cas9 Genome Editing Machinery Enabled by Nanoscale Zeolitic Imidazolate Framework. *J. Am. Chem. Soc.* **2018**, *140*, 143-146.

(9) WHO Model List of Essential Medicines. http://www.who.int/medicines/publications/essentialmedicines/20th_EML2017_FINAL_amendedAug2017.pdf?ua=1 (accessed 4 April 2018).

(10) Pan, Y. C.; Liu, Y. Y.; Zeng, G. F.; Zhao, L.; Lai, Z. P. Rapid synthesis of zeolitic imidazolate framework-8 (ZIF-8) nanocrystals in an aqueous system. *Chem. Commun.* **2011**, *47*, 2071-2073.

(11) Ragon, F.; Horcajada, P.; Chevreau, H.; Hwang, Y. K.; Lee, U. H.; Miller, S. R.; Devic, T.; Chang, J. S.; Serre, C. In Situ Energy-Dispersive X-ray Diffraction for the Synthesis Optimization and Scale-up of the Porous Zirconium Terephthalate UiO-66. *Inorg. Chem.* **2014**, *53*, 2491-2500.

(12) Cliffe, M. J.; Wan, W.; Zou, X. D.; Chater, P. A.; Kleppe, A. K.; Tucker, M. G.; Wilhelm, H.; Funnell, N. P.; Coudert, F. X.; Goodwin, A. L. Correlated defect nanoregions in a metal-organic framework. *Nat. Commun.* **2014**, *5*, 8.

(13) Maeda, H.; Tsukigawa, K.; Fang, J. A Retrospective 30 Years After Discovery of the Enhanced Permeability and Retention Effect of Solid Tumors: Next-Generation Chemotherapeutics and Photodynamic TherapyProblems, Solutions, and Prospects. *Microcirculation* **2016**, *23*, 173-182.

APPENDIX

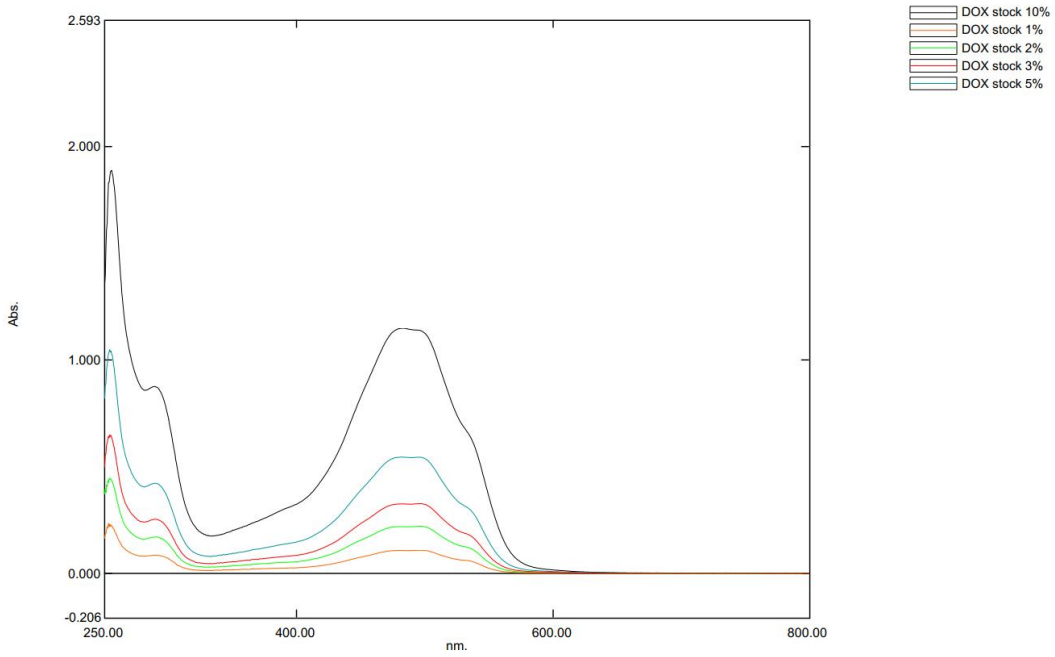

Figure 10. UV-Vis spectra of DOX stock solutions of varying concentrations used to calculate a calibration curve for DOX concentration.

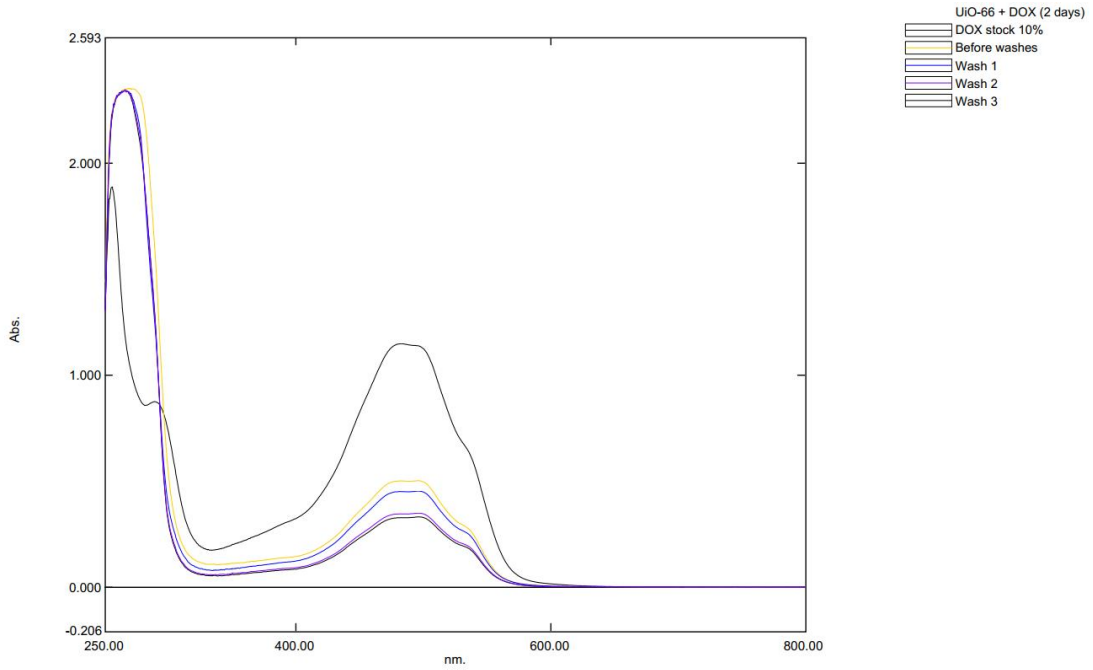

Figure 11. UV-Vis spectra of washes from UiO-66 two-day uptake of DOX.

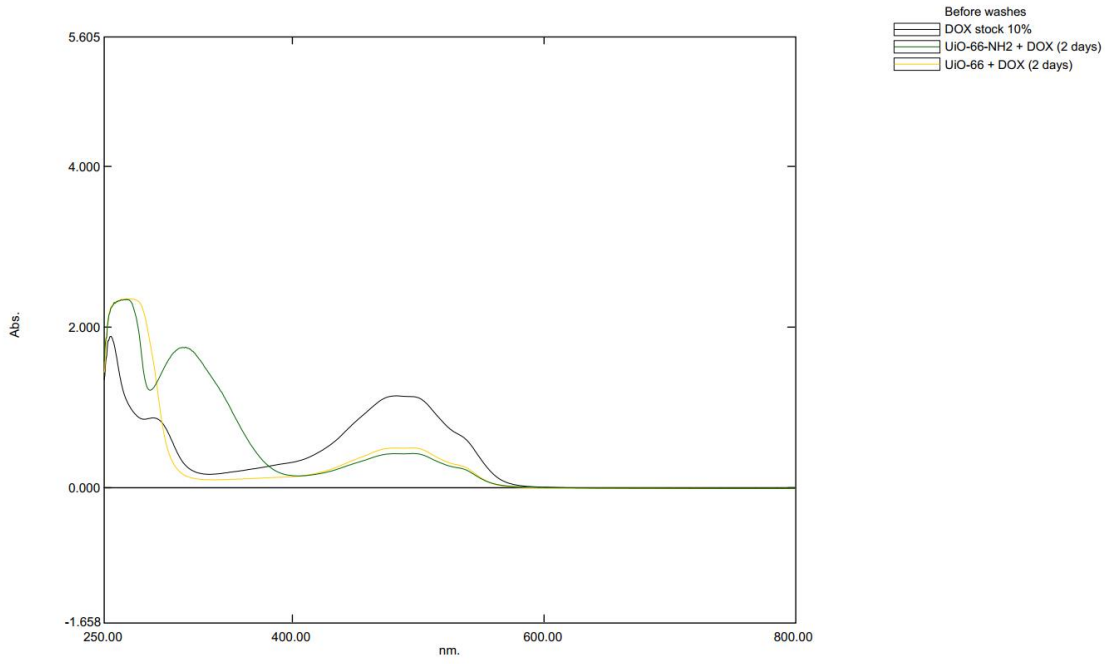

Figure 12. UV-Vis spectra of solutions from UiO-66 and UiO-66-NH_2 two-day uptakes of DOX.

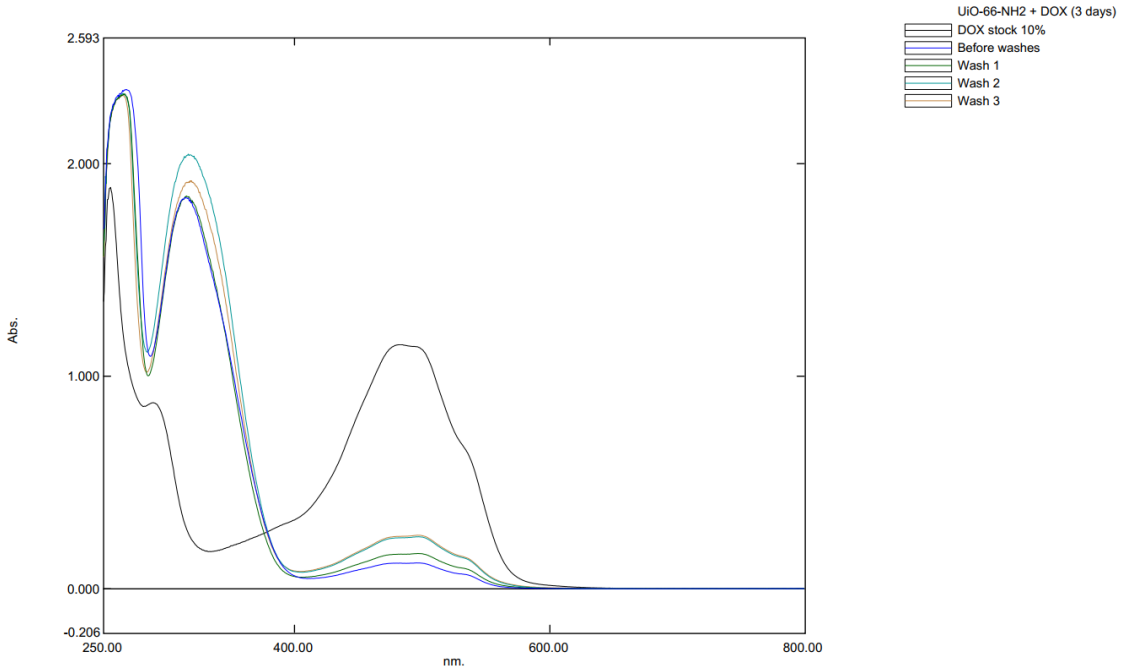

Figure 13. UV-Vis spectra of washes from UiO-66-NH_2 three-day uptake of DOX.

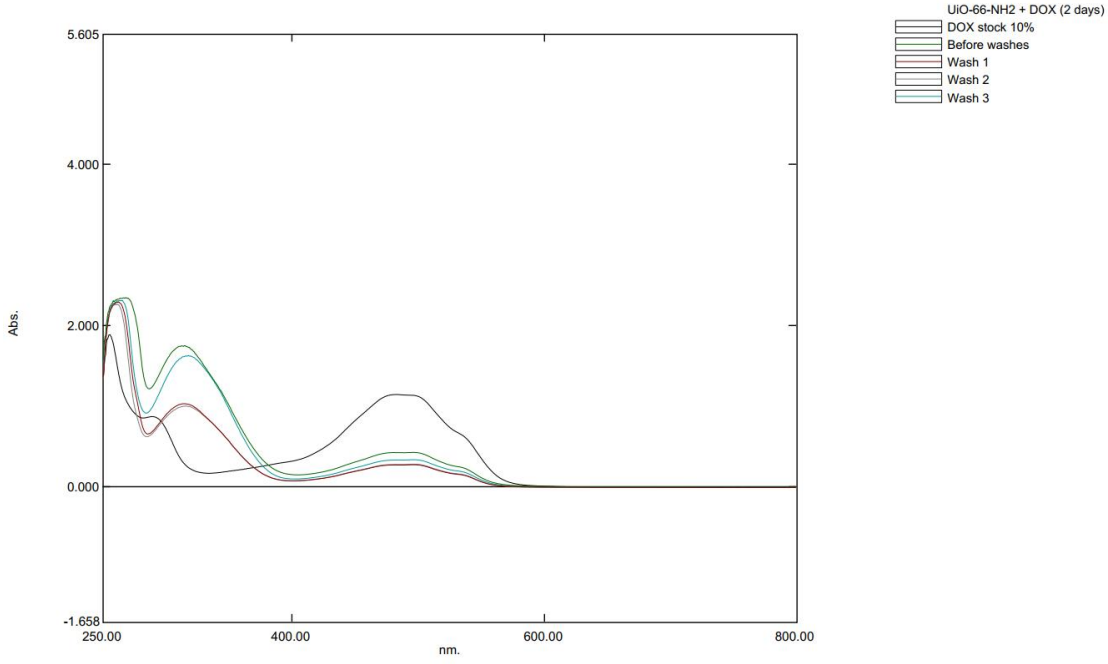

Figure 14. UV-Vis spectra of washes from UiO-66-NH_2 two-day uptake of DOX.

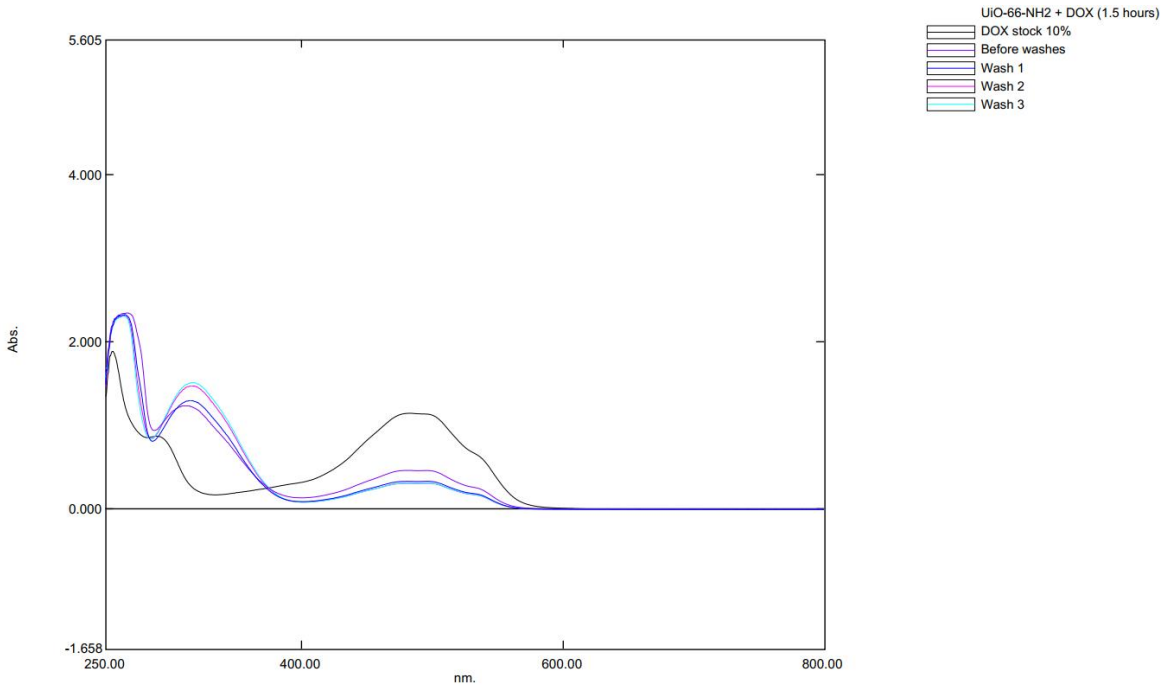

Figure 15. UV-Vis spectra of washes from UiO-66-NH_2 1.5 h uptake of DOX.

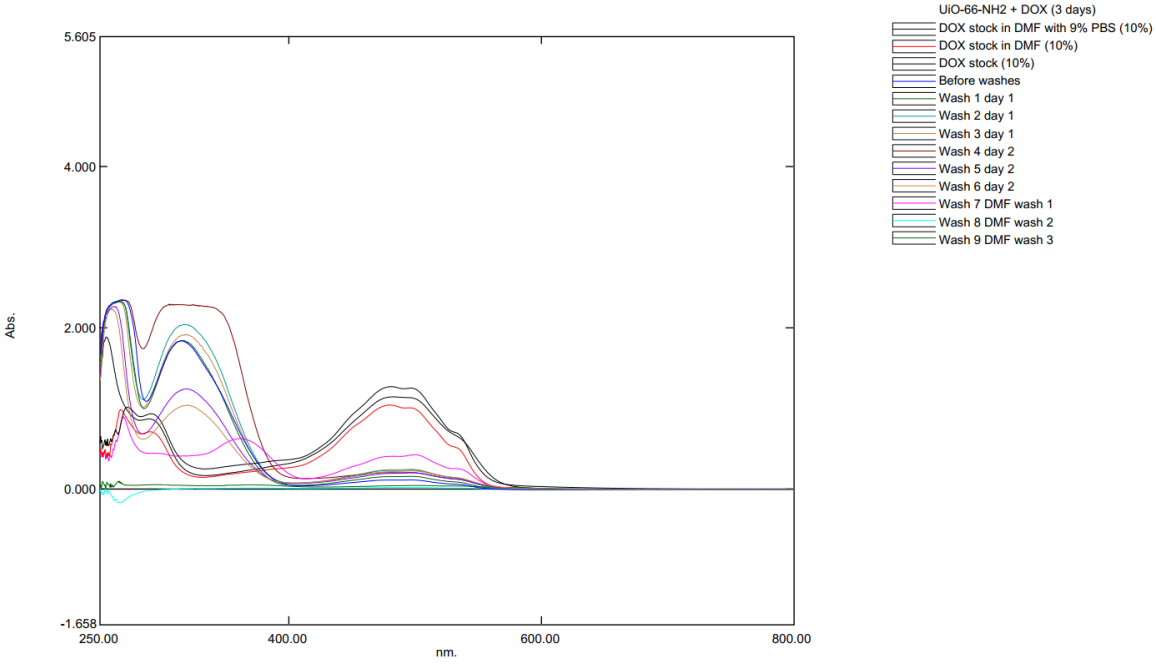

Figure 16. UV-Vis spectra of multiple days of washes from UiO-66-NH_2 three-day uptake of DOX.

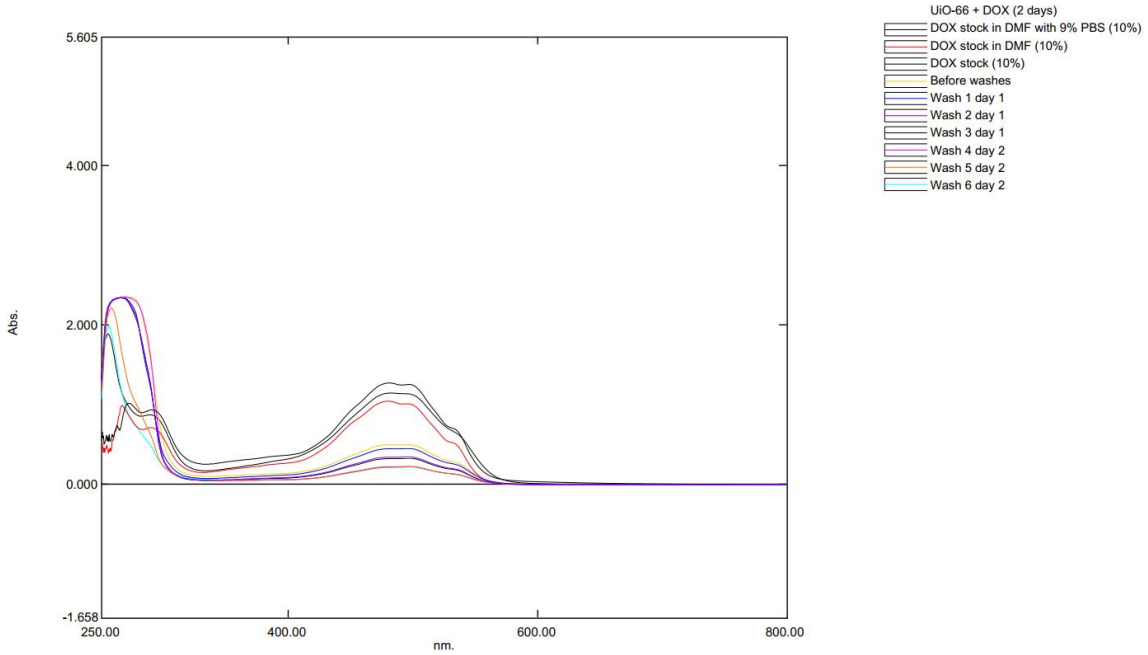

Figure 17. UV-Vis spectra of multiple days of washes from UiO-66 two-day uptake of DOX.